ABCM Symposium Series in Mechatronics - Vol. 1 - pp.48-57
Copyright © 2004 by ABCM

KINEMATIC CONTROL OF THE MAGELLAN-ISR MOBILE ROBOT

Altamiro Veríssimo da Silveira Júnior
Divisão de Engenharia Eletrônica, Instituto Tecnológico de Aeronáutica, Pça. Marechal Eduardo Gomes s/nº, 122228-900 São José dos Campos-SP
silveira@ele.ita.br

Elder Moreira Hemerly
Divisão de Engenharia Eletrônica, Instituto Tecnológico de Aeronáutica, Pça. Marechal Eduardo Gomes s/nº, 122228-900 São José dos Campos-SP
hemerly@ele.ita.br

Abstract. *A kinematic controller in Cartesian coordinates is proposed in this paper for application in mobile robot with differential driving. Lyapunov-like analysis is employed in the control system stability proof. Real time implementations and simulations results are also presented and discussed for the trajectory tracking and point stabilization cases. The performance of the controller is evaluated and compared with kinematic controller proposed by Kanayama.*

Keywords*. kinematic control, trajectory tracking, point stabilization, stability proof, mobile robot.*

1. Introduction

Recently, mobile robot control has attracted increasing interesting due to several potential applications in industry automation and other non-holonomic systems. This work considers trajectory tracking and point stabilization for mobile robot. In trajectory tracking, the robot should follow a reference trajectory with a specified velocity, while in point stabilization it should reach a specified point, following the shortest trajectory possible.

The usual approach in the literature consists in representing the real system by the kinematic model. This is a simplified model, which supposes perfect velocity tracking, i.e., robot dynamic, movement restrictions and external perturbations are not considered. In Kanayama et al. (1990), it is proposed a kinematic control law in cartesian coordinates for solving the trajectory tracking problem. In Souza (2000) a kinematic control law in polar coordinates was proposed. Convergence of the tracking error was shown for the case in which the distance between the guidance point and the symmetry point is null. When this distance is different from zero, only a local stability proof was presented. This control law is better suited for solving the point stabilization problem.

The goals of this paper are:

- Proposition of a kinematic control law in cartesian coordinates that should be able to solve the trajectory tracking and point stabilization problems, with stability proof of control system via the Lyapunov-like analysis (Slotine and Li, 1991).
- Performance comparison between the proposed control law and the that in Kanayama et al. (1990) by simulations using the Magellan-ISR mobile robot parameters.
- Real time performance evaluation of the proposed control law, by using the Magellan-ISR mobile robot, in both trajectory tracking and point stabilization cases.

This paper is organized as follows: In Section 2, the kinematic model in Cartesian coordinates is described and the control law proposed by Kanayama et al. (1990) is presented. The control law proposed in this work is deduced and the stability proof is presented using the Lyapunov-like analysis (Slotine and Li, 1991). In Section 3, simulations and real time results are presented and discussed. Finally, in Section 4, the conclusions are presented.

2. Kinematic control

Consider the Figure (1), in which the mobile robot C is represented by the coordinates $\mathbf{p}=[x_c \;\; y_c \; \theta \;]^T$ of the center of mass, moving over a plane with linear velocity v and angular velocity ω. The matrix equation that describes the kinematic model of mobile robot is given by

$$\dot{\mathbf{p}} = S\eta \tag{1}$$

or,

$$\begin{bmatrix} \dot{x}_c \\ \dot{y}_c \\ \dot{\theta} \end{bmatrix} = \begin{bmatrix} cos(\theta) & -d.sin(\theta) \\ sin(\theta) & d.cos(\theta) \\ 0 & 1 \end{bmatrix} \begin{bmatrix} v \\ \omega \end{bmatrix} \tag{2}$$

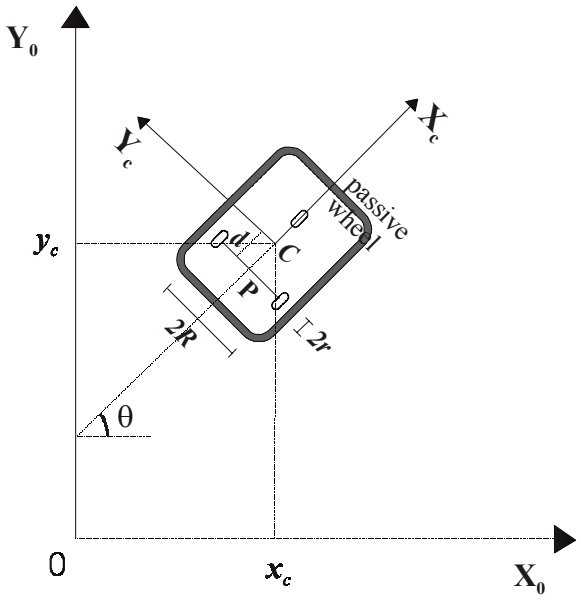

Figure 1. Mobile robot and system coordinates.

where the parameter d is defined as the distance between the guidance point C (center of mass) and the symmetry point P, η represents the velocity vector of robot and S, the matrix of kinematic model.

The kinematic control is defined by the vector

$$\mathbf{v}_c = \begin{bmatrix} v_c \\ \omega_c \end{bmatrix} = \begin{bmatrix} v \\ \omega \end{bmatrix} \tag{3}$$

supposing a null velocity error. The Figure (2) shows the diagram of the kinematic control in cartesian coordinates.

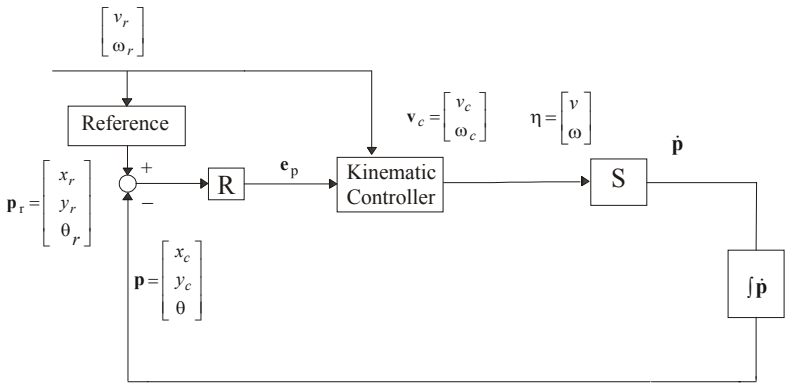

Figure 2. Diagram of kinematic control.

2.1. Kinematic Controller I

Consider the Figure (3), which the robot C, described in Fig.(1) by the coordinates $\mathbf{p}=[\, x_c \;\; y_c \;\; \theta \,]^T$ of the center of mass and by the velocity vector η, should track the reference robot R, also described by the Eq. (1), moving with linear velocity v_r and angular velocity ω_r, which position is given by the coordinates $\mathbf{p}_r = [\, x_r \;\; y_r \;\; \theta_r \,]^T$.

Let's define the posture tracking error vector $\mathbf{e}_p$ expressed in the basis of frame $\{C,X_c,Y_c\}$ as

$$\mathbf{e}_p = R(\theta)(\mathbf{p}_r - \mathbf{p}) \tag{4}$$

or

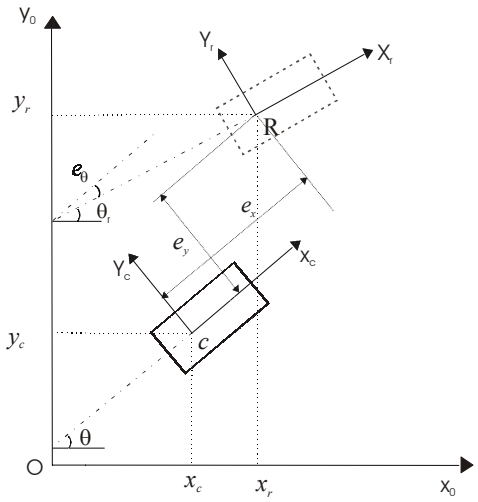

Figure 3. Mobile robot and reference robot.

$$\mathbf{e}_p = \begin{bmatrix} e_x \\ e_y \\ e_\theta \end{bmatrix} = \begin{bmatrix} cos(\theta) & sin(\theta) & 0 \\ -sin(\theta) & cos(\theta) & 0 \\ 0 & 0 & 1 \end{bmatrix} \begin{bmatrix} x_r - x_c \\ y_r - y_c \\ \theta_r - \theta \end{bmatrix} \tag{5}$$

where $R(\theta) = \begin{bmatrix} cos(\theta) & sin(\theta) & 0 \\ -sin(\theta) & cos(\theta) & 0 \\ 0 & 0 & 1 \end{bmatrix}$ is the rotation matrix.

Differentiating the Equation (5), yields

$$\begin{bmatrix} \dot{e}_x \\ \dot{e}_y \\ \dot{e}_\theta \end{bmatrix} = \begin{bmatrix} \omega.e_y - v + v_r cos(e_\theta) \\ -\omega.e_x + v_r.sin(e_\theta) \\ \omega_r - \omega \end{bmatrix} \tag{6}$$

The control law proposed by Kanayama et al. (1990), that provides asymptotic convergence of posture error when the parameter *d* is null, is given by

$$\mathbf{v}_c = \begin{bmatrix} v_c \\ \omega_c \end{bmatrix} = \begin{bmatrix} k_x .e_x + v_r.cos(e_\theta) \\ \omega_r + k_y v_r e_y + k_\theta .v_r .sin(e_\theta) \end{bmatrix} \tag{7}$$

where k_x, k_y e k_θ are positive constants defined in the design of kinematic controller. More details about the stability proof of this control law can de found in Kanayama et al. (1990). To ensure the stability of this control law, the linear reference velocity (v_r) should be positive. From Kanayama et al. (1990), the Lyapunov-like (Slotine and Li, 1991) time derivate function is given by

$$\dot{V}(e_x, e_y, e_\theta) = -k_x e_x^2 - \frac{v_r k_\theta sin^2(e_\theta)}{k_y} \leq 0 \tag{8}$$

In the specific case of point stabilization, there is no reference trajectory. So the linear and angular reference velocities (v_r and ω_r) are null. The robot should reach the reference point, following the shortest trajectory possible.

The control law given by Equation (7) guarantees good performance in the trajectory tracking case. However, in point stabilization, it presents serious restrictions. By replacing v_r and ω_r by zero in Equation (7), yields

$$\mathbf{v}_c = \begin{bmatrix} v_c \\ \omega_c \end{bmatrix} = \begin{bmatrix} k_x e_x \\ 0 \end{bmatrix} \tag{9}$$

which has no angular control and it is not able to reduce the component *y* (e_y) of posture error.

In the Section 2.2, it will be proposed another control law in cartesian coordinates that should be able to solve the trajectory tracking and point stabilization problem.

2.2. Kinematic Controller II

The controller proposed in this work employs the frame system used in Del Río (1997), where the posture tracking error vector $\mathbf{e}_p$ is calculated in the reference robot frame system. More precisely, $\mathbf{e}_p$ is expressed in the frame $\{R,X_R,Y_R\}$ in Fig. (4).

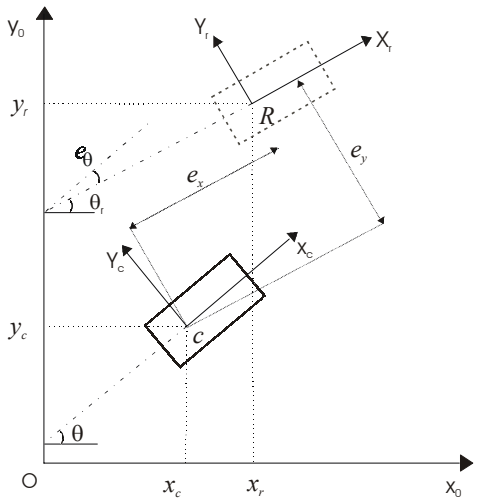

Figure 4. Mobile robot and reference robot.

$$\mathbf{e}_p = R(\theta_r)(\mathbf{p} - \mathbf{p}_r) \tag{10}$$

or,

$$\mathbf{e}_p = \begin{bmatrix} e_x \\ e_y \\ e_\theta \end{bmatrix} = \begin{bmatrix} cos(\theta_r) & sin(\theta_r) & 0 \\ -sin(\theta_r) & cos(\theta_r) & 0 \\ 0 & 0 & 1 \end{bmatrix} \begin{bmatrix} x_c - x_r \\ y_c - y_r \\ \theta - \theta_r \end{bmatrix} \tag{11}$$

where $R(\theta_r) = \begin{bmatrix} cos(\theta_r) & sin(\theta_r) & 0 \\ -sin(\theta_r) & cos(\theta_r) & 0 \\ 0 & 0 & 1 \end{bmatrix}$ is the rotation matrix.

Differentiating the Equation (11), yields

$$\begin{bmatrix} \dot{e}_x \\ \dot{e}_y \\ \dot{e}_\theta \end{bmatrix} = \begin{bmatrix} \omega_r e_y - v_r + v.cos(e_\theta) \\ -\omega_r e_x + v.sin(e_\theta) \\ \omega - \omega_r \end{bmatrix} \tag{12}$$

Considering the parameter d null, the asymptotic convergence of posture error can de obtained using the control law,

$$\mathbf{v}_c = \begin{bmatrix} v_c \\ \omega_c \end{bmatrix} = \begin{bmatrix} v_r cos(e_\theta) - \Im_{xy}^{-1} e_x cos(e_\theta) - \Im_{xy}^{-1} e_y sin(e_\theta) \\ \omega_r + \frac{e_x v_r}{A_\theta^2}.\frac{sin^2(e_\theta)}{e_\theta} - \Im_\theta^{-1} e_\theta - \frac{e_y v_r}{A_\theta^2}.cos(e_\theta).\frac{sin(e_\theta)}{e_\theta} \end{bmatrix} \tag{13}$$

where A_θ, $\Im_{xy}$ e $\Im_\theta$ are positive constants, defined as controller gains.

For stability proof via Lyapunov-like analysis (Slotine and Li, 1991), consider the function V

$$V(e_x,e_y,e_\theta)=\frac{1}{2}(e_x^2+e_y^2)+\frac{1}{2}\mathrm{A}_\theta^2 e_\theta^2 \tag{14}$$

which is bounded from below by zero. Differentiating the Equation (14), and using the Eq. (12) and (13), we get

$$\dot{V}(e_x,e_y,e_\theta)=-\Im_{xy}^{-1}(e_x cos(e_\theta)+e_y sin(e_\theta))^2 - \Im_\theta^{-1} A_\theta^2 e_\theta^2 \leq 0 \tag{15}$$

which is negative semi-definite.

From Equation (14) and (15), e_x, e_y and e_θ are bounded. Differentiating the Equation (15), we verify that $\ddot{V}(e_x,e_y,e_\theta)$ is also bounded. By using the Barbalat Lemma (Slotine and Li, 1991), it follows that $\dot{V}(e_x,e_y,e_\theta)$ converges to zero. Hence, e_x and e_θ converge to zero. Applying the Barbalat Lemma (Slotine and Li, 1991) in Eq. (12) it follows that e_y also converges to zero (Silveira, 2003). It should be stressing that the Kanayama et al. (1990) $\dot{V}(e_x,e_y,e_\theta)$ only depends on e_x and e_θ, whereas in Eq. (15) it also depends the e_y. In simulations and real time applications, it will be clear the effect of this difference in the convergence behaviour.

3. Real time implementations and simulations results

To illustrate the theoretical results present in the previous Section, it will be evaluated and compared the performance of the two control laws for trajectory tracking and point stabilization. The simulations were performed in MATLAB 5.3 and the real time applications are implemented in MOBILITY software, version 1.0 (IS Robotics, 2000). The distance between the guidance point and symmetry point was calculated experimentally and results in d = 0.02 m.

The Magellan mobile robot used here for the real time applications is shown in Fig. (5).

Figure 5. Magellan mobile robot.

It was considered the same conditions in real time implementations. The Euler method was employed for equation integration with time step T=0.1 s. The norm of linear and angular velocity control was limited respectively in $|v_c| \leq 1.0$ m/s and $|\omega_c| \leq 2.0$ rad/s. To avoid prohibitive control effort in transient period, it was used a linear saturation in signals velocities control with time derivate equal to 0.3 for v_c and 0.5 for ω_c.

In simulations algorithms, it was introduced an white noise (τ_v) modeling by a gaussian distribution with zero mean and a specific variance ($N(0;\sigma^2)$) in velocity signal (v and ω) to reproduce the conditions of real case and verify the robustness of each control law. The velocity error is defined as

$$\mathbf{e}_c=\begin{bmatrix} e_v \\ e_\omega \end{bmatrix}=\begin{bmatrix} v_c - v \\ \omega_c - \omega \end{bmatrix} \tag{16}$$

For performance evaluation, 20 realizations were employed for calculating the mean and variance of the control signals (v_c and ω_c). For fair performance comparison of the two kinematics controllers, the gains of each controller were adjusted to obtain an equivalent effort control in the transient period. Two different sets of results are considered: a) typical realization showing the behaviour of all relevant variables (posture and velocity errors), and b) the statistical (mean and variance) of the control signals. In the figures and table the following convention is used:

- Kinematic controller I – KI.
- Kinematic controller II – KII.

3.1. Trajectory tracking

For the trajectory tracking case, it was considered a reference trajectory with linear and nonlinear segments, which v_r = 0.4 m/s, ω_r= 0, ± 1.5 rad/s and the initial position of reference trajectory $\mathbf{p}_r$=(0.5,0,π/2). The robot starts with initial condition **p**=(0, 0, 0). The controllers gains and the disturbances can be found in Tab. (1). It was defined the mean posture error $\bar{e}_m$ as

$$\bar{e}_m = \frac{1}{t_{final}} \int_0^{t_{final}} (e_x^2(t) + e_y^2(t) + e_\theta^2(t))dt \tag{17}$$

where t_{final} is the final time of simulation or real time case. Initially, consider the simulation case, whose results are presented in Fig. (6), (7) and (8).

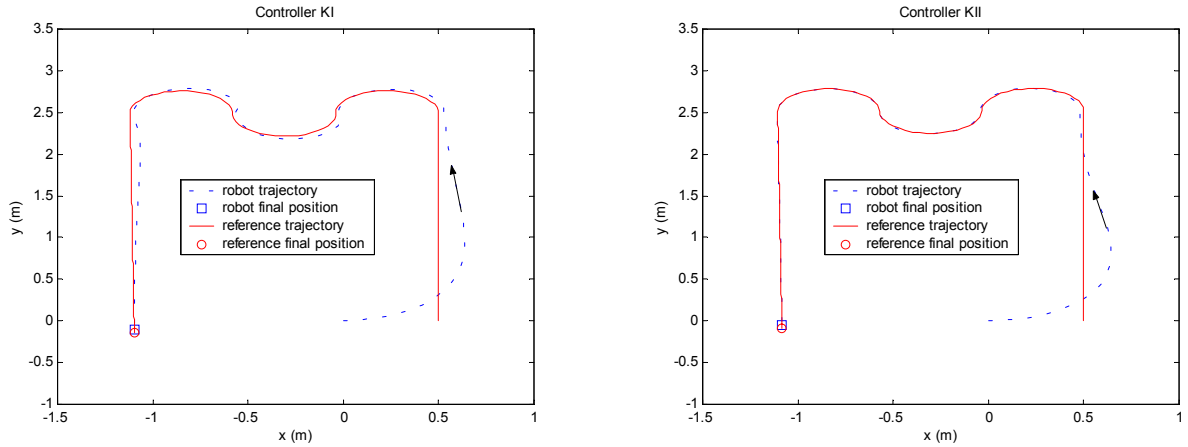

Figure 6. Robot and reference trajectories for controllers KI and KII.

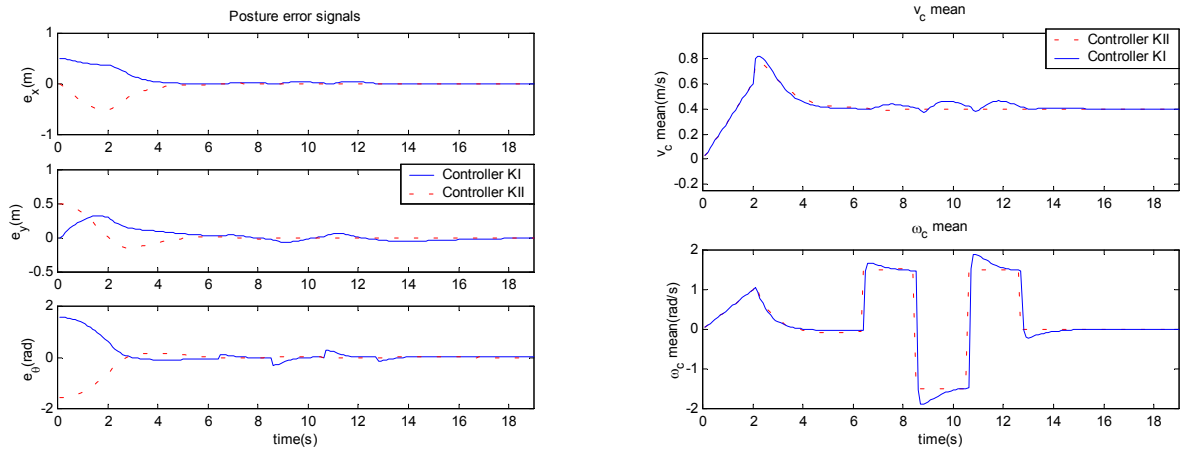

Figure 7. Posture error signals and mean control signals for controllers KI and KII.

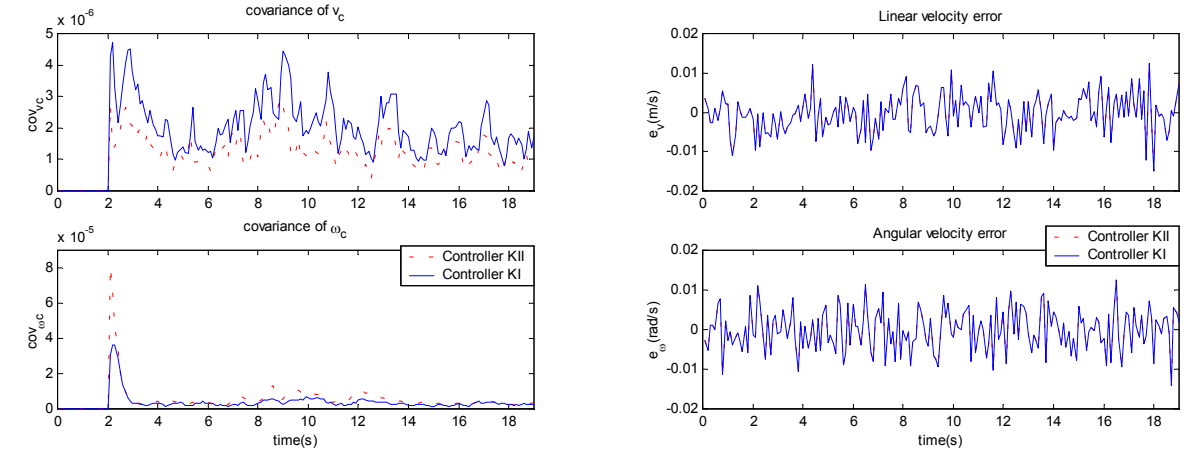

Figure 8. Covariance of control signals and velocity error signals for controllers KI and KII.

Comparing the mean posture error $\bar{e}_m$ of two controllers in Tab. (1), we can verify that the performance of the controllers KII was slightly better than that of controller KI. From Figure (6), we can verify that the controller KII exhibits an improvement in the convergence behaviour due to the influence of the y error component (e_y) in time derivate of $V(e_x,e_y,e_\theta)$ given by Eq. (14). However, from Figure (8), we note that the angular control covariance of controller KII is larger than controller KI in the transient period.

We now consider the real time case. The robot velocities are achieved differentiating the signal position provided by odometer. The results are presented in Fig. (9), (10) and (11).

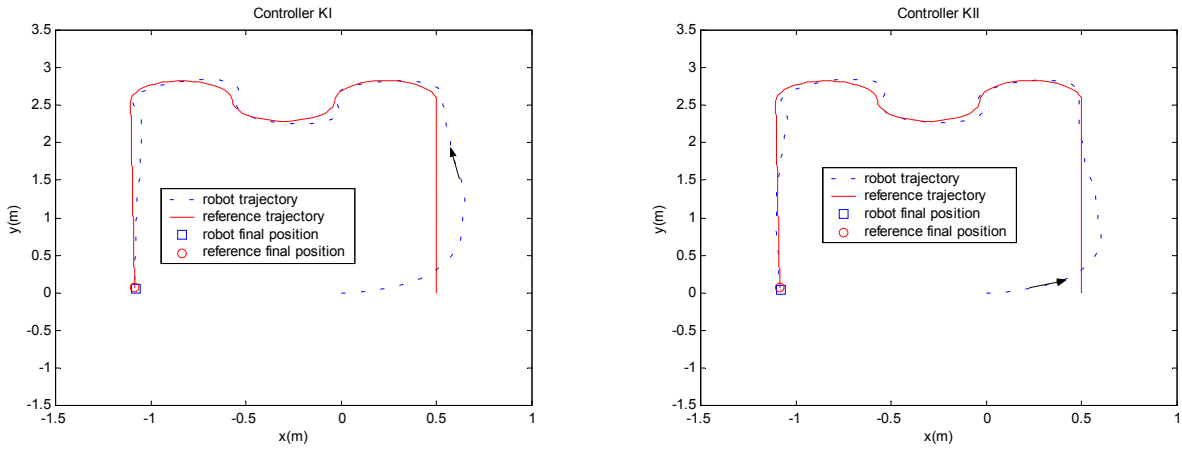

Figure 9. Robot and reference trajectories for controllers KI and KII.

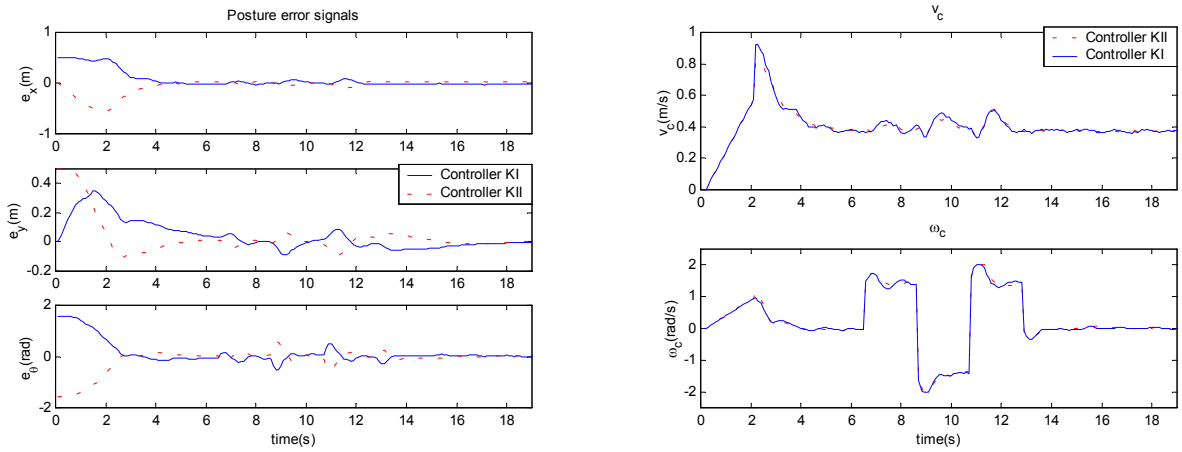

Figure 10. Posture error signals and velocities control signals for controllers KI and KII.

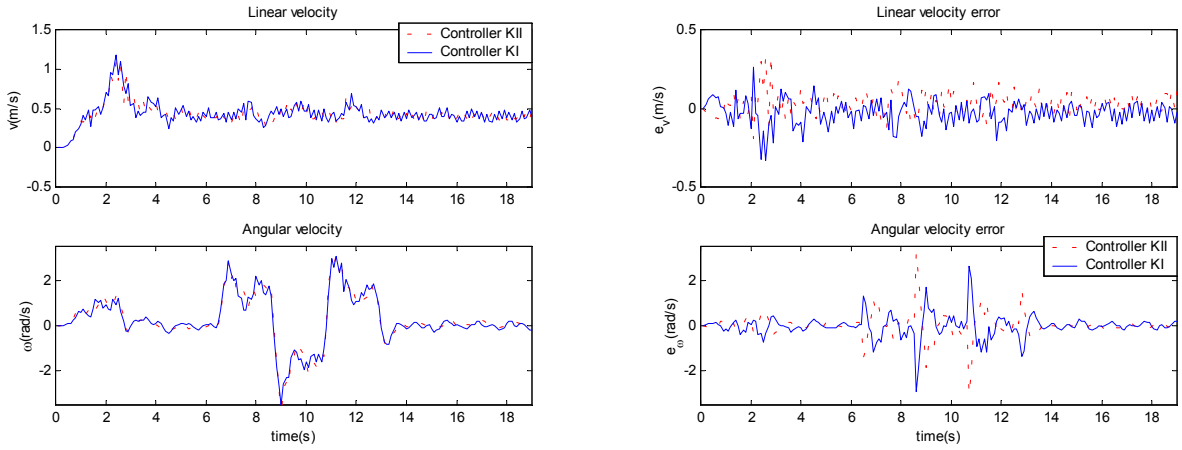

Figure 11. Linear and angular velocities signals and velocities error signals for controllers KI and KII.

As in the simulation results, we verify that the mean posture error $\bar{e}_m$ of controller KII was slightly smaller than controller KI. The controller KII provided an improvement in the convergence process, when compared to controller KI. Both controllers had sufficient robustness to compensate the effect of velocity errors and variation in the parameter *d*, which was supposed null in the design of the kinematic controller.

3.2. Point stabilization

It was considered the reference point $\mathbf{p}_r=(1,1,\pi/2)$. The robot starts with initial condition $\mathbf{p}=(0,0,0)$. The controllers gains and the disturbances can be found in Tab. (1). Initially, consider the simulation, as shown in Fig. (12), (13) and (14).

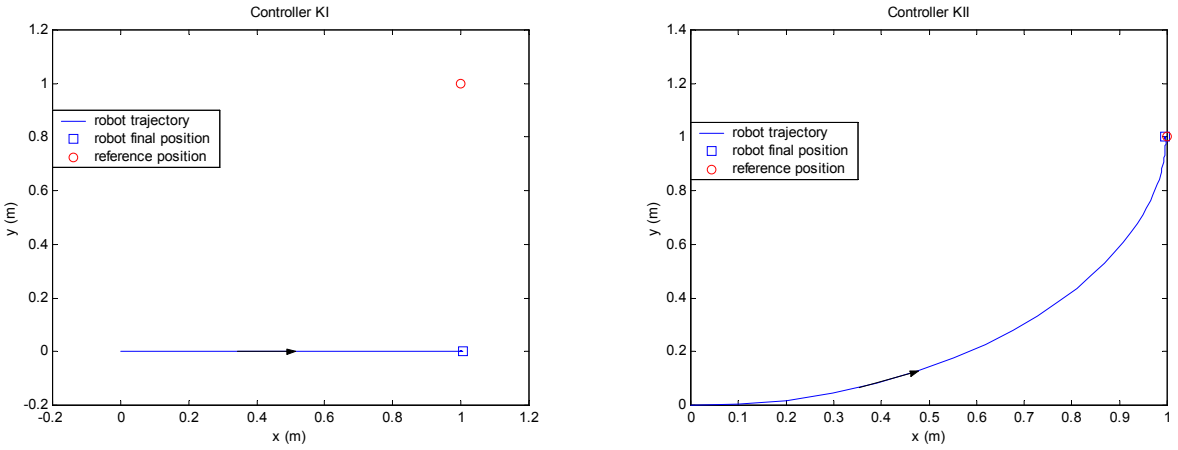

Figure 12. Robot trajectories for controllers KI and KII.

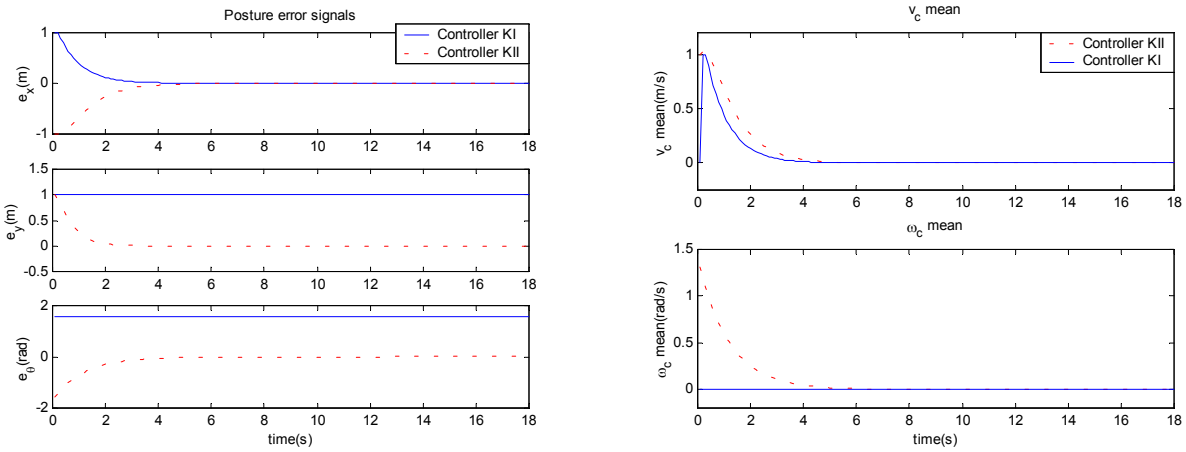

Figure 13. Posture error signals and mean control signals for controllers KI and KII.

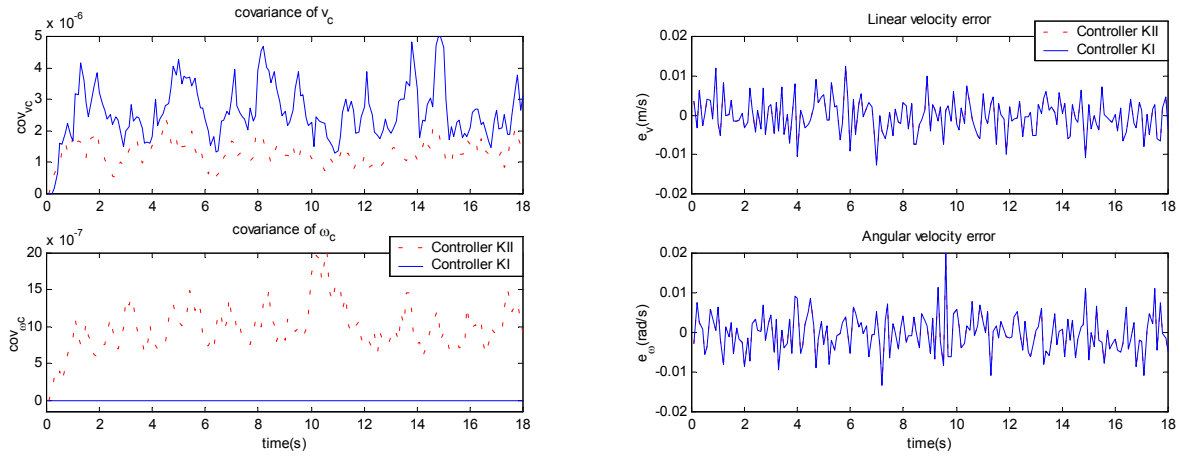

Figure 14. Covariance of control signals and velocity error signals for controllers KI and KII.

As expected, from Figure (12) we conclude that the controller KI was not able to reach the reference point, moving only along the direction x. On the other hand, the controller KII was able to stabilize in the specified reference point.

We now consider the real time case, as indicated in Fig. (15), (16) and (17).

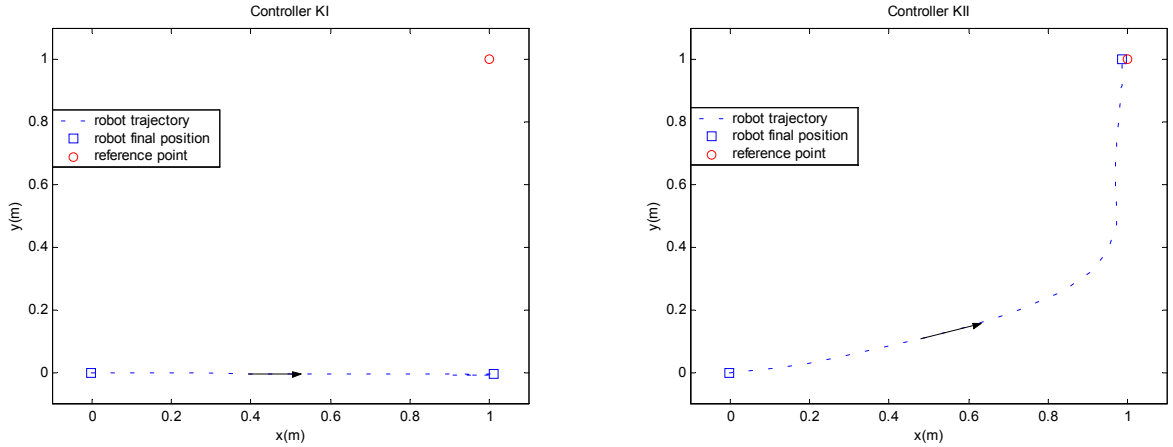

Figure 15. Robot trajectories for controllers KI and KII.

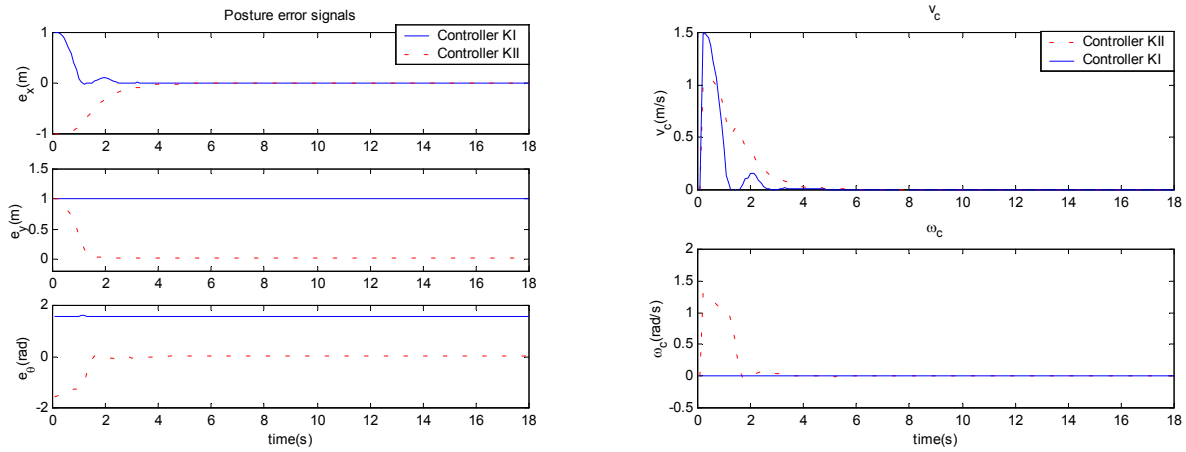

Figure 16. Posture error signals and control signals for controllers KI and KII.

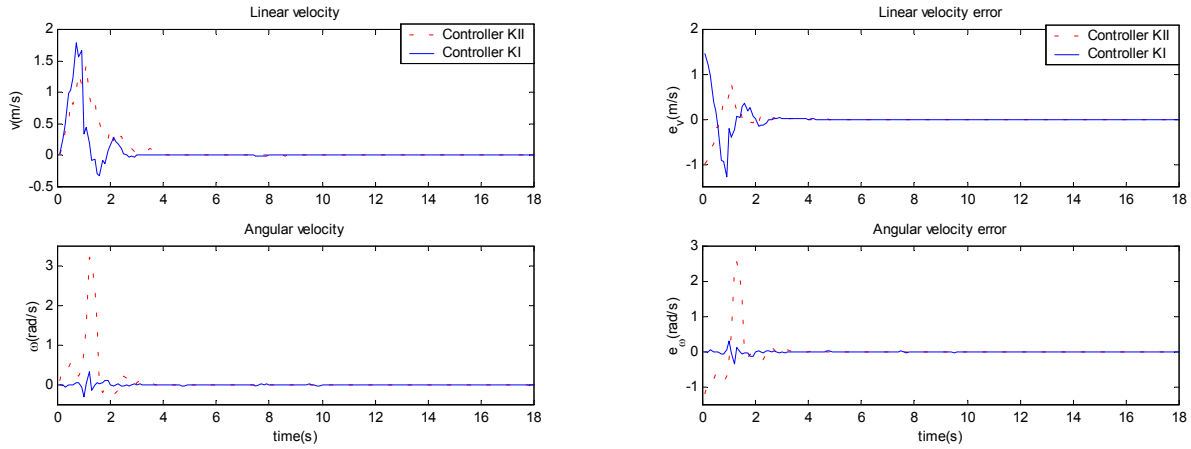

Figure 17. Linear and angular velocities signals and velocities error signals for controllers KI and KII.

The results in Figures (15), (16) and (17) are coherent with that obtained in simulations. As expected, the controller KI compensates only for the error in the component x. The controller KII can reach the specified point, thereby ensuring convergence of posture error. Table (1) contains all the controllers gains, mean posture error and disturbances.

Table 1. Kinematics controllers gains, mean posture error and velocity noise.

Figure	$\Im_{xy}$	$\Im_\theta$	A_θ	k_x	k_y	k_θ	τ_v	$\bar{e}_m$ (KI)	$\bar{e}_m$ (KII)
(6)	1.0	1.0	0.4	1.25	3	3	$N(0;2.5\text{x}10^{-5})$	0.2147	0.2124
(9)	1.0	1.0	0.4	1.25	3	3	–	0.2451	0.2444
(12)	1.0	1.2	0.4	1.	3	3	$N(0;2.5\text{x}10^{-5})$	–	–
(15)	1.0	1.29	0.4	1.5	3	3	–	–	–

4. Conclusions

A kinematic control law for mobile robots was proposed in this work. Cartesian coordinates were used, and the frame system proposed in Del Río (1997) was employed. The stability proof was based on a Lyapunov-like analysis (Slotine and Li, 1991). Both simulation and real time results are presented. Moreover, the proposed controller is compared with that in Kanayama et al. (1990), for trajectory tracking and point stabilization problems. The controllers gains were adjusted experimentally, so as to provide smooth and fast transient response.

It was verified that both controllers have sufficient robustness to compensate the effect of parameter variation d and velocity error $\mathbf{e}_c$. It worth pointing out that the full compensation of the velocity error would require a dynamic controller, which is far more complicated than the kinematic controller used here. Hence, this work indicates that when the external perturbations and disturbances are not severe, the performance of kinematic controller is satisfactory.

5. Acknowledgement

The authors thank Atech and CCSIVAM for the support.

6. References

Del Río, F.D, 1997, “Analysis and evaluation of mobile robot control: application to electric wheelchairs”, Ph.D Universidade de Sevilla, PhD Thesis.

IS Robotics, 2000, Magellan Pro Compact Mobile Robot User’s Guide.

Kanayama, Y., Kimura, Y., Miyazaki, F. and Noguchi, T., 1990, “A stable tracking control method for an autonomous mobile robot”, IEEE Int. Conf. on Robotics and Automation, Vol.1,pp. 384-389.

Silveira, A. V. J., 2003, “Controle cinemático e dinâmico de robôs móveis”, São José dos Campos:ITA, MSc Thesis.

Slotine, J. J. E., Li, W., 1991, “Applied nonlinear control”, New Jersey: Prentice Hall.

Souza, C. J., 2000, “Controle adaptativo de robôs móveis”, São José dos Campos: ITA, MSc Thesis.